



On-site determination of an uncommon cracking mechanism due to composition gradients in a nickel steel weld



J. Booman^{a,*}, P.G. Fazzini^b, José Luis Otegui^c

^a Universidad Nacional de Rosario, Av. Pellegrini 250, S2000BTP Rosario, Argentina

^b GIE S.A., 52 Galicia, 7600 Mar del Plata, Argentina

^c Y-TEC (YPF – CONICET), Baradero 777, Ensenada, Argentina

ARTICLE INFO

Article history:

Received 10 July 2015

Received in revised form 8 October 2015

Accepted 6 November 2015

Available online 7 November 2015

Keywords:

3% Ni steel

Weld

Cracking

Thermal fatigue

ABSTRACT

This article analyzes a 3.5% Ni steel cryogenic cylindrical vessel, after the detection by non-destructive inspection of cracks in a circumferential weld. Possible in-service damage mechanisms are discussed, in particular, vibration, low cycle thermal fatigue and hydrogen embrittlement. On-site experimental analysis allowed defining that cracks were due to a manufacturing problem. A final weld bead with much greater concentration of Ni generated an uncommon mechanism of thermal fatigue. In Ni alloyed steels, small variations of Ni around 36% involve variations of almost an order of magnitude in the coefficient of thermal expansion. Proposed actions for integrity assurance of the vessel and lessons learned for fabrication of future vessels are briefly discussed.

© 2015 Elsevier Ltd. All rights reserved.

1. Introduction

This article originates in a failure analysis of cracks found in the shell-to-cap circumferential weld of a 2440 mm diameter, 82 mm thick cryogenic vessel at a petrochemical complex, Fig. 1. All studies were performed on site, during a programmed plant stop. Two vessels with the same characteristics and operational history were operated at the facility, but only one presented discontinuities.

This horizontal, cylindrical vessel with semispherical heads was manufactured in 1978; specified base metal for shell and cups is SA 203 Gr. E, a ferritic pearlitic steel alloyed with 3.5% nickel [1]. Stress relieving post weld heat treatment was done according to ASME VIII, parts UW-40, UCS-56 and UCS 65 [2]. Welds were also completely radiographed. Pre-operational hydrostatic testing was performed at 115 bar. Maximum design working temperature and internal pressure are 101 °C and 77 bar, respectively. Specified minimum mechanical properties are 275 MPa yield strength and 20% elongation, with a UTS between 485 and 620 MPa, minimum specified chemical composition is detailed in Table 1.

The vessel has a 140 mm thick polyurethane insulation, and is used as a liquefied gas separator, prior to shipping to expander valves. Normal operational conditions are – 60 °C, 58 bar internal pressure. The process gas is C1+ and is composed of methane, ethane, propane, butane and gasoline. It is a “dry” gas, water content is 0.16 ppm, with a pH between 3.3 and 4.1. The content of hydrogen sulfide in gas is 0.000165% and the content of carbon dioxide (CO₂) is 0.54%.

Fig. 2 shows the record of pressures during 2011 and 2012. This vessel was taken out of service, on average, 6 times per year. At scheduled stops the temperature rise up to room temperature was very slow, at a rate of 0.4 °C/min, but could be up to 2 °C/min during unscheduled stops. Cooling rates during commissioning again were always controlled below a maximum of 0.3 °C/min.

* Corresponding author.

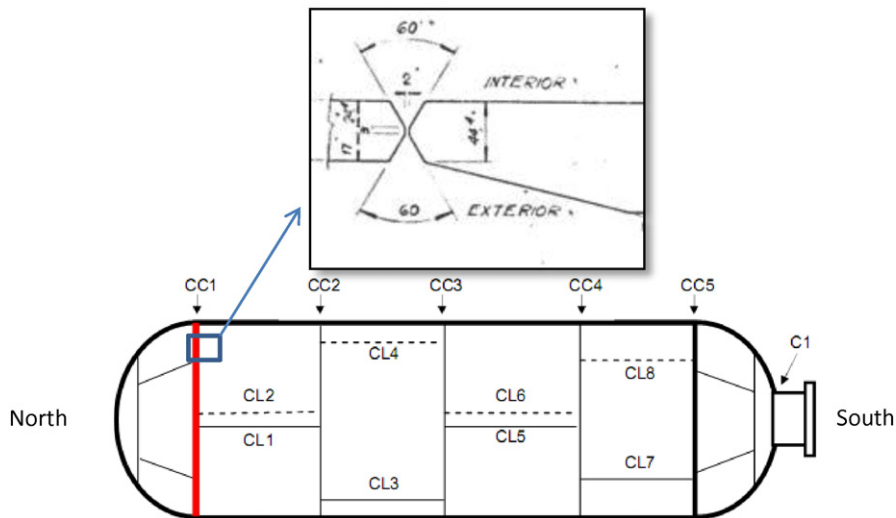


Fig. 1. Cracked vessel. Inset: detail of the Cap – surround welded joint.

There are no records of inspections since reception up until 2010, since the vessel had been classified as of low risk. In 2010 nondestructive testing (NDT) was performed, and cracks were detected in one of the cap to shell circumferential welds. These cracks were small and mainly in the direction of the weld, i.e. circumferential to the vessel, and were repaired by grinding. During inspection carried out two years later, cracks were found again, this time spread in different directions [3].

Documents containing specific information about the MMA (manual metal arc) welds are not available. Electrodes recommended for welding this SA 203 Gr E steel are C2-S8016 [4], C2-S8018 or ENiCrFe-2 [5]. Pure weld metal chemical compositions for each are presented in Table 2. Note that the first two have a composition similar to the base material, while the third contains a high content of nickel and chromium. Table 3 shows pure weld metal mechanical properties corresponding to each electrode.

2. In-situ metallographic analysis

As mentioned, circumferential cracks in the weld of the North cap detected during the NDT inspection carried out in 2010 were eliminated by grinding. Evidence of the indications was not kept. During the NDT inspection in 2012 in. penetrant testing, chemical analysis, hardness and field metallography were used to identify the new cracks detected. All these techniques were used “in situ”, directly on the component during the plant stop. This time, cracks were in different directions. Fig. 3(a) shows the detected mid-weld cracks, as detected by penetrant ink.

Hardness of most of weld material is 150 to 170 HB, similar to the hardness of shell base metal. But very high hardness was detected at specific sites, with values between 330 and 415 HB. These sites were subsequently identified by chemical etching with Nital 10% and the presence of two dissimilar materials was identified: one, susceptible to etching, and the other, non-susceptible. Immune areas to Nital etching are delimited in Fig. 3(b) [3].

In situ chemical analysis of these areas detected three materials with different compositions:

1. Base material, with a nickel content between 1.5 and 5.5%.
2. Metal of “normal” weld metal, with a content of Ni between 3 and 3.75%.
3. Non-susceptible filler material to etching, with high hardness.

Composition of region 3 corresponds to electrodes E8018-C2 or E8016-C2, as recommended for this steel type [6]. Detected cracks were all located in weld metal, on the edge of zones 2 and 3, on the side of the harder material. In these hard areas contents of Ni of up to 7.5% and of Cr up to 12.5% were found. Zn was also detected in both weld metals.

This high Ni and Cr material can correspond to an electrode of the type ENiCrFe-2, which provides a pure weld metal with 70% Ni and 15% Cr [5]. This type of weld metal is commonly recommended for welding 3.5% nickel alloy steel, but it is noticed that when using austenitic stainless steel electrodes, the coefficient of expansion must be kept in mind [7]. It is estimated that in this case it was used to perform a repair during the construction stage.

Table 1
Chemical composition of 203 SA Gr. E steel.

C	Mn	P	S	Si	Ni
≤0.23	≤0.8	≤0.035	≤0.04	0.15–0.4	3.25–3.75

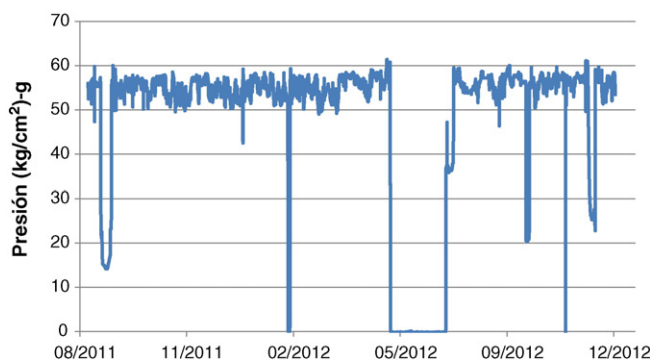


Fig. 2. Pressure cycles during last year and a half of service.

Metallographic replicaes at several intersections between the etched and un-etched regions are shown in Fig. 4. In all cases cracks occur at the interface of both materials, mostly on the side of un-etched weld material. Pictures at the left show areas without cracks, while cracked areas are shown at the right. The quality of the replicaes does not allow clear identification of the microstructure of the weld materials. However, the etched material is compatible with a typical ferritic–bainitic weld metal, while the un-etched material is most probably an austenitic stainless. [8].

One notable shortcoming of these replicaes is that the differentiation between transgranular and intergranular crack paths is not quite clear. The component was repaired and returned to service immediately after these in-situ analyses, so no further experimental evidence was available afterwards.

3. Analysis of possible damage mechanisms

The failure analysis included the evaluation of all damage mechanisms to which the vessel could have been exposed, according to API RP 571 [9]. All possible mechanisms were grouped according to the type of evidence required: susceptibility of weld materials, aggressive agents, location and morphology of defects, sufficiency of static and cyclic stress levels.

The nondestructive evaluation described in the previous section gave enough evidence to discard most of the mechanisms. Graphitization, spheroidization, temper embrittlement, strain aging, high temperature corrosion, creep, and embrittlement at 475 °C could be ruled out since their occurrence requires high temperature for long periods of time, and the vessel has not been subjected to these conditions. Although high temperatures are reached during the manufacturing process they were kept for short times.

Due to the absence of the aggressive agent, damage due to a steam blanketing, liquid metal embrittlement, caustic SCC (stress corrosion cracking) and ammonia SCC could be discarded. Even though the gas contains chlorine, nickel alloys have high resistance to chlorine SCC, so this mechanism could also be ruled out.

On the other hand, the location and/or morphology of the damage are not compatible with the following mechanisms: erosion, erosion corrosion, cavitation, brittle fracture, localized or generalized loss of thickness, and short term overheating. Corrosion-fatigue can be ruled out, since no corrosion products were left. Thermal shock can be ruled out as well, since this mechanism would not explain why the cracks are concentrated in weld metal.

According to the external visual inspection carried out in 2010, cracks were also found in the concrete subfloors. This could be a product of vibrations transmitted by the vessel, so with the available information at the time it was not possible to rule out a mechanism of vibration-induced fatigue. But again, the cracks are neither placed near supports or any stress concentration that could be related with the transmission of gravitational loads, nor with piping systems.

Cracking in welded dissimilar materials occur during operation at high temperature, between the ferritic and the austenitic weld metals, but cracks in this case should be concentrated in the ferritic side [11].

Reheating cracking can occur due to stress relaxation during post weld heat treatments, or during service at high temperatures. If the cracking had occurred as a result of the heat treatment of subsequent passes, the cracks would not be found on austenitic metal, but on the material of the previous weld passes, which are ferritic.

Table 2

Chemical composition of electrodes for SA 203 Gr. E steel welds.

Electrode	C	Mn	P	S	Si	Ni	Cr	Mo	Fe	Cu	Nb + Ta	Co
S8016-C2	0.06	0.9	0.011	0.006	0.5	3.2	–	–	–	–	–	–
S8018-C2	0.07	1.12	0.015	0.007	0.32	3.45	–	–	–	–	–	–
ENiCrFe-2	0.1	1–3.5	0.03	0.02	0.75	>62	13–17	0.5–2.5	≤12	≤0.5	0.5–3	≤0.12

Table 3

Mechanical properties of electrodes for SA 203 Gr. E steel welds.

Electrode	Yield strength (MPa)	Ultimate tensile strength (MPa)	Elongation (%)	Heat treatment
S8016-C2	530	630	30	605 °C × 1 h, S.R
S8018-C2	572	648	22	
ENiCrFe-2	1034	1158	15	Oil quenched and tempered at 425 °C

The likelihood of mechanical fatigue can be assessed on the basis of service pressure cycles (Fig. 2). There are two main cycle amplitudes. The larger pressure range is in the order of 60 bar (peak to peak), indicative of operation outages. Operating pressure cycles are in the order of 10 bar.

In a thin-walled cylinder, the principal stresses are hoop (circumferential) and axial (longitudinal) stresses, which are well known:

$$\sigma_{\text{axial}} = \frac{PD}{4t} \quad \sigma_{\text{hoop}} = \frac{PD}{2t}$$

Where P is the pressure, D is the shell outer diameter and t is wall thickness.

The stress cycles that could have generated fatigue propagation of the cracks in the cup circumferential weld can then be identified as:

- Operation stop and start cycles of 90 MPa (hoop) and 45 MPa (axial), that is, less than the third part of the yield strength of the vessel material.
- In-service cycles of 45 MPa (hoop) and 22 MPa (axial).

Both conditions lead to very low cyclic stress conditions, below the fatigue limit of the base material. This allowed discarding the mechanism of mechanical fatigue due to pressure cycles [10]. On the other hand, the circumferential component of the cyclic

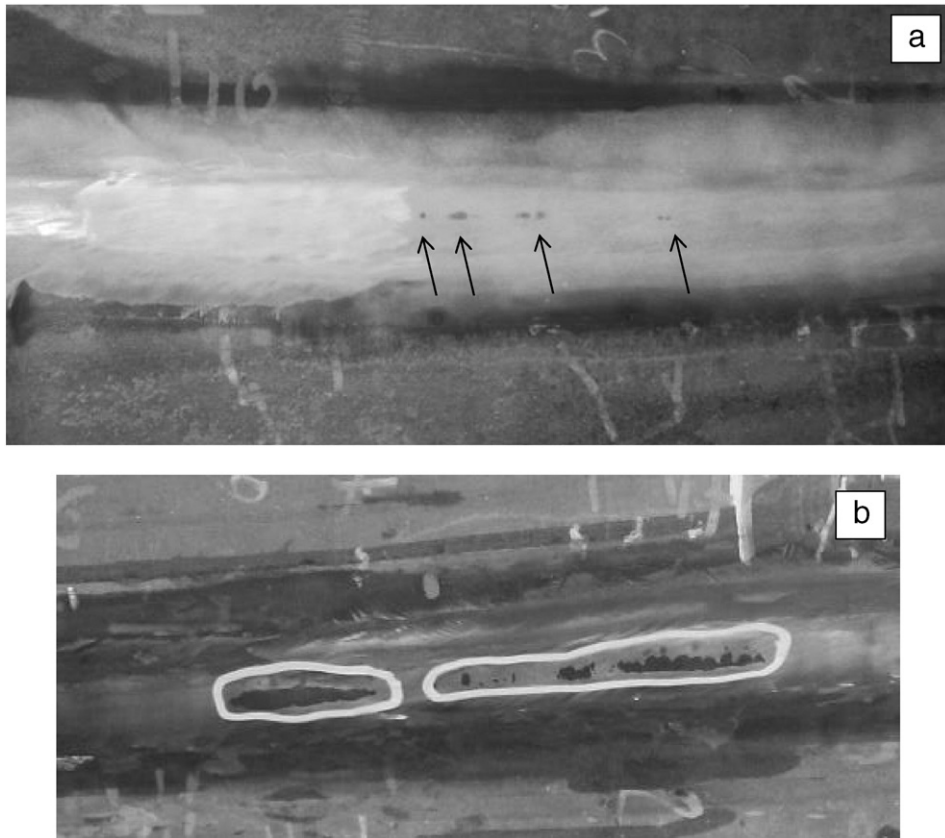


Fig. 3. a) Mid-weld cracks, as detected by penetrant ink, b) after Nital etching, immune areas are delimited.

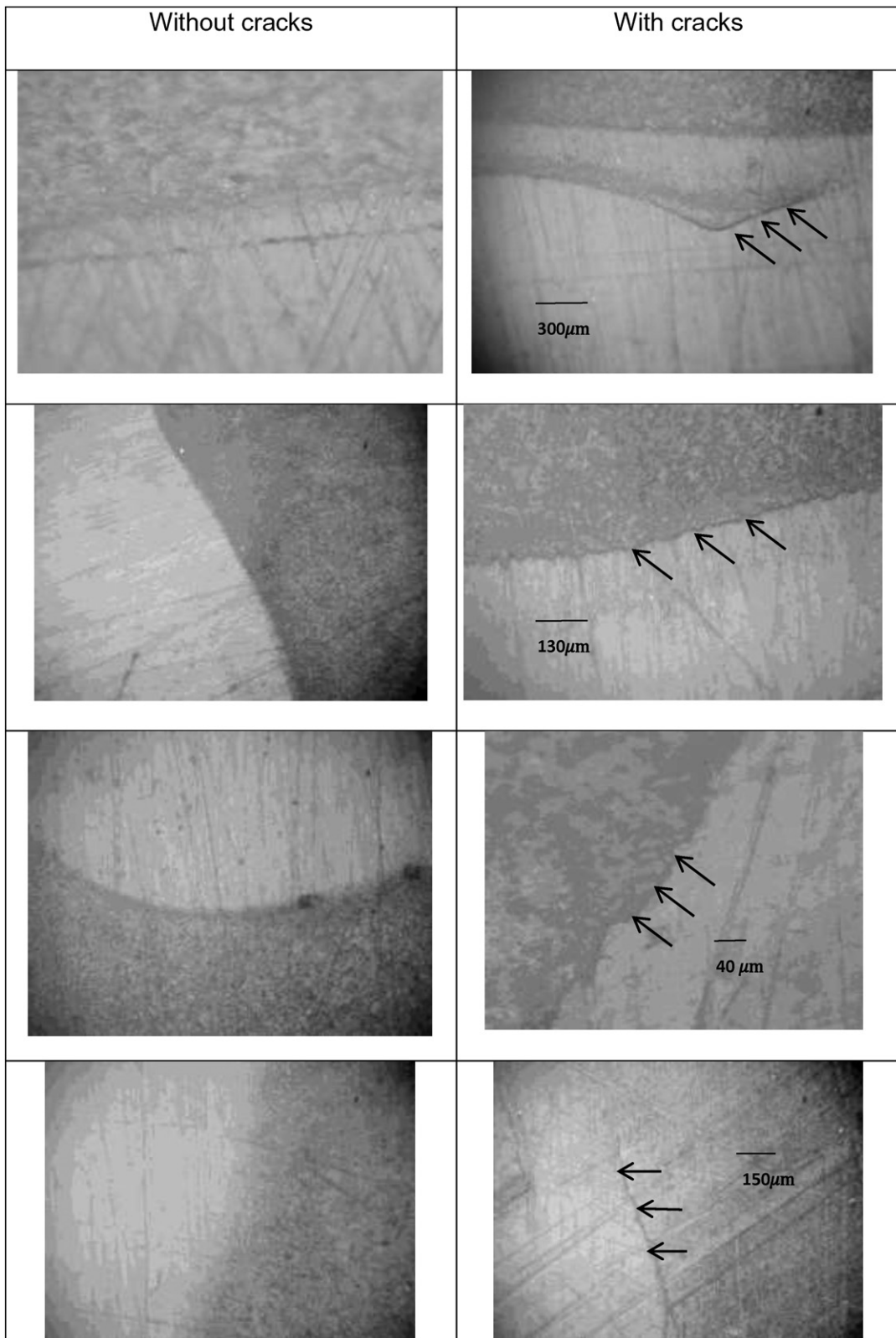


Fig. 4. Metallographic replicas at the intersection of both weld filler materials.

stresses due to internal pressure is twice the longitudinal component, so this mechanism would have triggered cracks with preferably longitudinal orientation, in both the seam and girth welds in the shell. But cracks are concentrated in only one of the cup welds in particular.

The presence of the interface between chemically and microstructurally very dissimilar materials could lead to large differences in mechanical and thermal properties, which were studied in detail. It was found that in the case of nickel alloys, the analyzed conditions could have resulted in a mechanism of thermal fatigue. Thermal fatigue is similar to mechanical fatigue, but in this case, cyclic stresses are not originated by mechanical loads but by differences in expansions and/or contraction between different parts of the component, when it is subjected to steep temperature variations. This mechanism is discussed in what follows.

4. Proposed damage mechanism due to gradient in composition

Fig. 5 [11] shows the variation of the coefficient of thermal expansion of nickel containing steels/alloys. There is a sharp decline for a certain Ni% range, reaching a minimum of 10^{-6} for an alloy with 36% Ni. This alloy is known as INVAR (that comes from “invariant”) and has great technological importance for applications requiring alloys that do not become deformed with temperature. This discovery earned Charles Guillaume a Nobel prize in 1920.

Consider an E NiCrFe-2 weld metal, which provides 70% of Ni (Table 2). If this electrode is used for the recap or repair of a weld previously welded with a low Ni electrode, and neither further weld passes nor heat treatment are carried out afterwards, it is reasonable that a large composition gradient between adjacent weld beads would remain. According to the dilution of the high-nickel weld metal into the low Ni previous passes, areas in the weld metal with nickel values close to the invar composition (36% Ni) can be expected. This is sketched in Fig. 6(a, b).

In this case, as the temperature lows down for operation, zones 1, 2, 3 and 5 in Fig. 6a contract. Since the high Ni material is forced to deform along with the surrounding low Ni weld and base metals, compression stresses will be generated in area 4 and tensile stresses in areas 3 and 5.

In areas subjected to traction (zones 3 and 5), high tensile thermal stresses would be added to the operating stresses (due mainly to internal pressure). Under these conditions, it is likely that added stresses would be sufficient to produce plastic strains during each heat cycle, and even cracking after few cycles.

From Fig. 3 it is seen that the difference in thermal expansion of INVAR is larger with respect to materials with lower Ni content (zone 3), than with a material with a higher Ni content. Zone 3 depicts where the cracks were actually detected, Fig. 3.

Consider an extreme case in which the 3.5% Ni weld metal (Table 2) is surrounded by Invar. Fig. 5 defines a difference of thermally induced strain of the order of $20 \times 10^{-6} K^{-1}$. Considering a thermal cycle in each service outage of the order of 120 K, a maximum differential deformation “ ϵ ” of the order of 2400×10^{-6} is obtained. Some part of this strain would be accommodated as elastic displacements, since the INVAR portion of the weld is not fully restrained by its surrounding low Ni environment.

If the volume of the “repaired” area is small, especially through the thickness dimension (Fig. 6b), this high Ni area would be forced to deform accompanying the material surrounding it, so the interface between zones 4 and 5 of Fig. 4 would see high stresses of thermal origin. Assuming a condition of plane strain, the apparent rigidity of the material is 1.1 E and hence the maximum possible thermal stress is:

$$\sigma = 1.1 E \epsilon = 1.1 \times 210.000 \times 2400 \times 10^{-6} = 554 \text{ MPa.}$$

This value is added to the applied stress due to internal pressure, resulting in a mostly biaxial stress with axial components in the order of 650 MPa. This simple model allows predicting maximum stresses above the material's strength. Actually, predicted

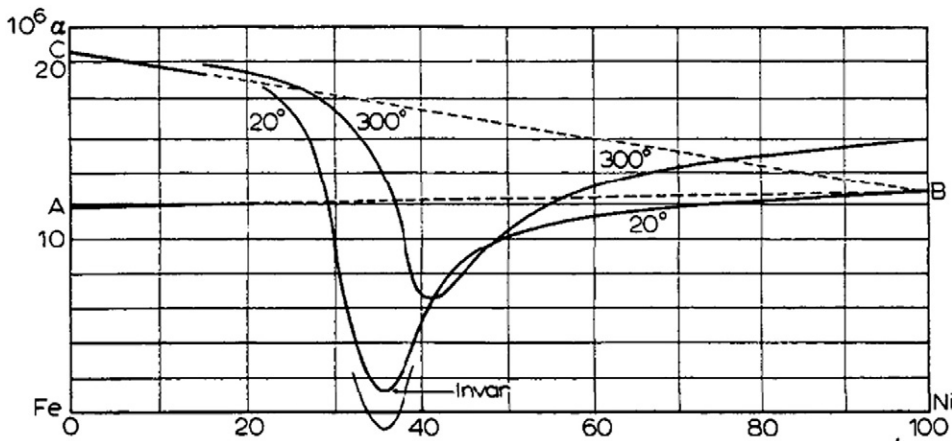


Fig. 5. Variation of coefficient of thermal expansion upon nickel content.

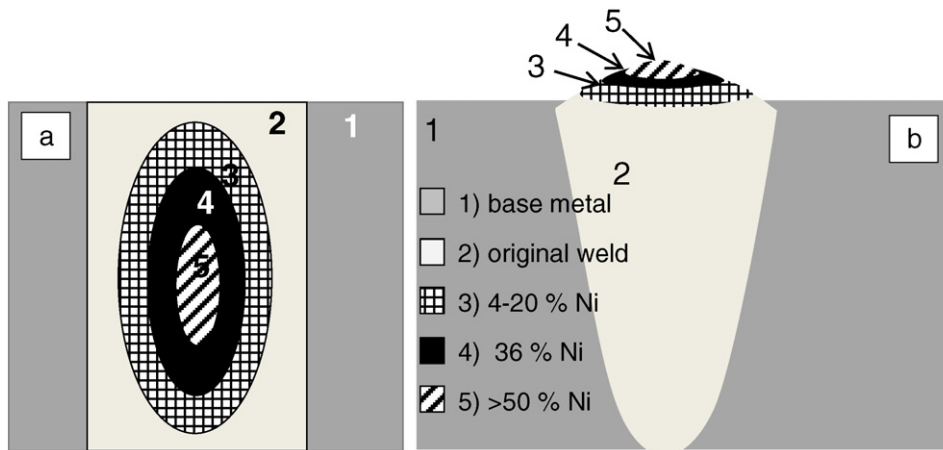


Fig. 6. Schematic of gradients of chemical composition in the cap weld: (a) on the outer surface, (b) through-thickness.

stresses are larger than twice the minimum specified yield strength for the base material of the vessel. These are stress cycles during service outages. Added to them are residual welding stresses, which are usually of yield point magnitude [12]. Regions 3, 4 and 5 in Fig. 6 are small volumes within weld metal in the central region of the “reinforcement”. Both transverse and longitudinal components of weld residual stresses can be considered as purely tensile. Residual stresses are static, do not add to the stress cycles, but are tractive in the cracked region and add to the maximum stress in each loading cycle.

The ideal “shakedown” model of a locally plastic strained material surrounded by a purely elastic material predicts that if the amplitude of the local applied stress cycle exceeds yield stress, the material deforms plastically. When the load is removed, the elastic contraction of the bulk forces the small, highly strained area to return to its initial dimensions, generating a local field of compressive (plasticity induced) residual stresses that impedes plastic yielding during future cycles. If the applied stress exceeds twice the yield stress, there is local yielding also when unloading to room temperature. In this way, each load and temperature cycle would produce plastic deformation, giving rise to the phenomenon of low cycle thermal fatigue or ratcheting [13].

Approximately six cycles per year of full start and stop cycles have been estimated, adding up to about 200 cycles from construction until 2010. Once material ductility was exhausted, it is possible that with only 10–12 cycles since 2010, cracks would have reappeared in 2012.

Pure weld metal with ENiCrFe 2 filler material possesses high yield strength (around 1000 MPa, Table 2), which would make the occurrence of this phenomenon in the hard area difficult. But such properties are reached after quenching and tempering of the as-welded material, and for the composition of pure filler material. Metallographic evidence (Fig. 3) indicates that crack propagation occurred in areas where the composition is the result of the dilution with base metal and previous S8018-C2 weld passes. Specifications do not mention any heat treatment, rather than stress relief, so it is expected that the strength of the resulting material is much less than 1000 MPa.

Fig. 7 shows the Schaeffler diagram [14], which defines likelihood of damage mechanisms depending on the composition of Ni and Cr alloyed steels. The compositions of alternative filler materials are identified. The dotted line indicates all possible compositions of ECrNiFe 2 filler metal diluted with former passes (S8018 C2 and C2 S8016). The line passes through two risk areas: hot cracking and cold cracking, but does not extend through the zone of Sigma phase embrittlement, so that this mechanism can be discarded. Hot cracking can also be discarded, since it would have been detected during fabrication and, on the other hand, it cannot explain the reappearance of the cracks in 2012.

Cold cracking occurs due to loss of ductility in weld or heat affected base metals, the presence of high stress, generally residual, and the presence of diffusible hydrogen. Although actual dilution in our case is unknown, cold cracking can clearly occur at dilutions resulting in 20% equivalent nickel or less. According to chemical analyses, Ni in “repaired” metal does not exceed 7.5%, so this mechanism cannot be ruled out.

Cracks are located in austenitic weld metal, Fig. 3. Although hydrogen cracking is usually not as important in austenitic steels as is in ferritic steels, some nickel alloys are susceptible to this mechanism [15]. On the other hand, the dissolution of hydrogen in austenite is much greater than in ferrite, so most of the available hydrogen would diffuse into the austenite, enhancing embrittlement in austenite [16]. Fig. 8 [17] shows that this mechanism is active throughout the operating temperature range, and during outages (room temp.).

The introduction of hydrogen in weld metal could have occurred during manufacturing (welding) or during previous service. H₂ uptake during service is not considered likely since the process gas is dry, but service and maintenance records are not complete and it is not possible to rule out the possibility of a repair with an ENiCrFe-2 electrode contaminated with moisture early in the service life of the component.

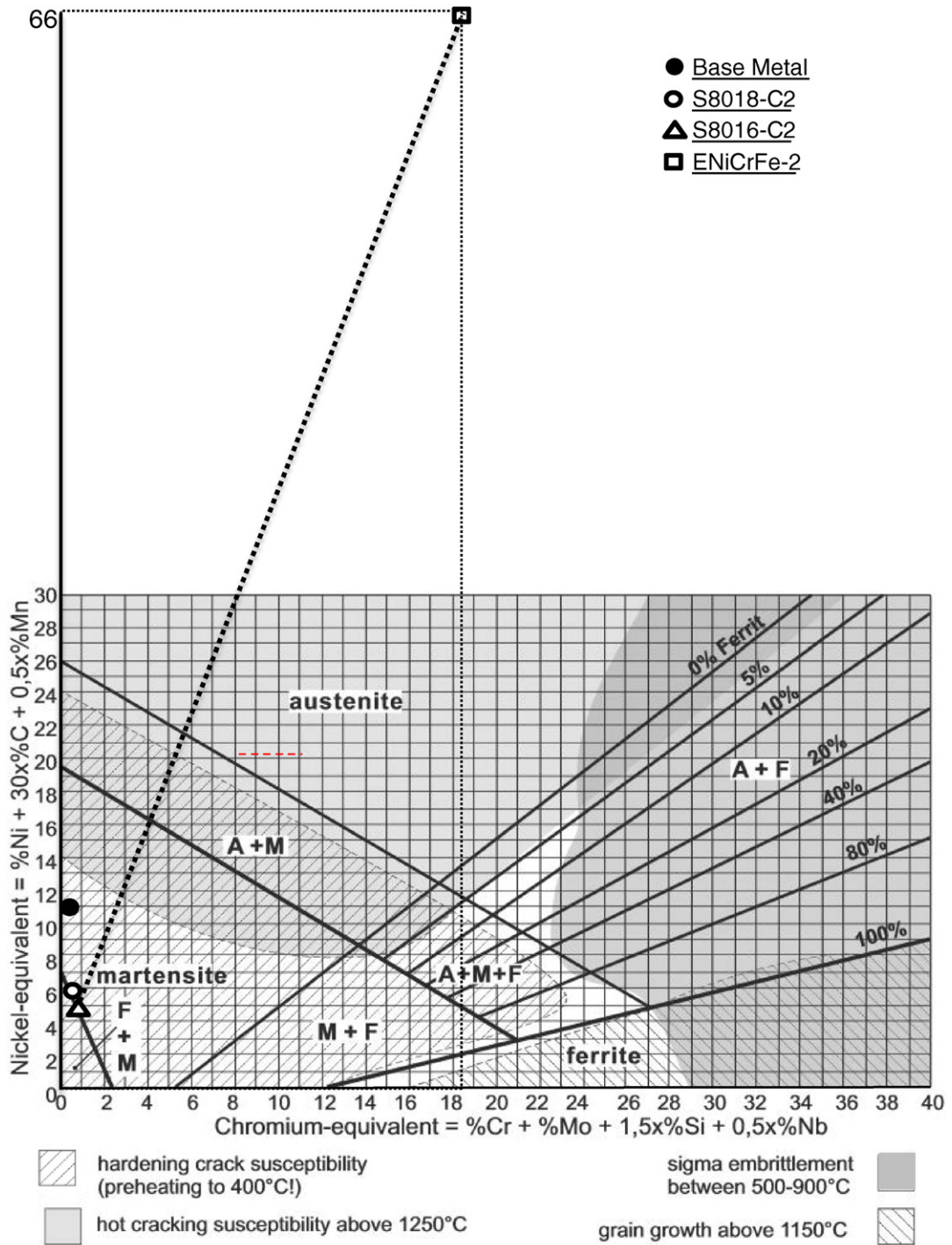


Fig. 7. Schaeffler diagram of possible weld metal compositions.

5. Relevant results for the future integrity of the component

All damage mechanisms proposed by API RP 571 were analyzed and most were discarded upon load conditions, operating temperature, susceptibility of the materials involved, the presence of aggressive agents and location and morphology of damage. This assessment did not allow discarding two mechanisms: hydrogen embrittlement and low cycle thermal fatigue.

Thermal fatigue mechanism was probably originated from a peculiarity that certain nickel alloys present: around 36% nickel, small variations of Ni may involve variations in the coefficient of thermal expansion of almost an order of magnitude. Hydrogen

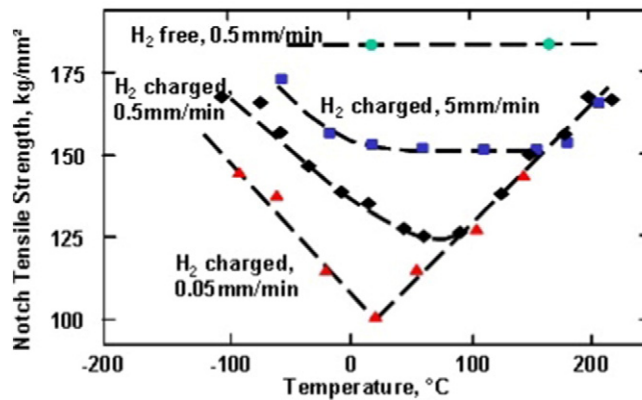


Fig. 8. Effects of temperature and hydrogen content on the impact strength of Ni steel.

embrittlement was probably due to poorly handled electrodes used in the repair pass, which were contaminated with moisture, and lack of post weld heat treatment that would have facilitated subsequent diffusion of absorbed hydrogen.

Common root cause for these two acting mechanisms has been the use of an ENiCrFe-2 electrode for the repair weld. This electrode is suitable for welding the base metal of the shell and cap, and advisable for the first passes, because in this case:

- heat cycles from the following passes temper previously deposited material, improving its mechanical properties.
- dilution in subsequent passes decreases gradients of chemical composition.
- heat cycles from the following passes allow diffusion of hydrogen.

Its use as a last pass, on the other hand, must be avoided.

The results of this study allowed predicting the recurrence of this cracking problem, since repairing the weld by grinding, as was done, does not necessarily remove the mechanism of nucleation and propagation of cracks. Future service cycles would re-nucleate and propagate cracks. Therefore, a strategy was agreed on actions to be taken during the next scheduled stop:

- Repeat mapping of chemical composition and high quality metallographic replica, using reagents that allow revealing austenitic microstructures, and delimit the areas of dissimilar microstructure.
- Grind out dissimilar weld material and measure remaining thickness.
- Where the resulting thicknesses are insufficient, repair the weld with a MMA procedure using low-hydrogen, low-nickel electrodes.
- Perform a post repair heat treatment to allow the diffusion of the hydrogen trapped in the weld metal.

6. Conclusions

The failure analysis described in this article was carried out during a scheduled plant outage, without the aid of laboratory chemical and metallographic analysis, since it was not possible to extract samples. The possible mechanisms of in service degradation were analyzed on the basis of standard non-destructive inspection, hardness measurements and field metallography. Even with these restrictions, it was demonstrated that chemical inhomogeneity in the weld bead of one of the vessel caps generated an uncommon damage mechanism that led to crack growth by thermal fatigue, probably combined with hydrogen embrittlement.

This damage mechanism was due to a repair weld carried out with a high Ni electrode, and originated in a peculiarity shown by certain nickel alloys: around 36% nickel, small variations of Ni may involve variations of almost an order of magnitude in the coefficient of thermal expansion. The mechanism of hydrogen embrittlement was probably due to the repair weld carried out with an electrode contaminated with moisture, and the lack of any post weld heat treatment.

Acknowledgments

This research work was partly funded by CONICET (Consejo Nacional de Investigaciones Científicas y Técnicas de la República Argentina, Grant PIP 00193/12), Agencia de Promoción Científica (Argentina, Grant PICT 0582/10), and Universidad Nacional de Rosario, Argentina. Authors thank Gie S.A. Integrity of Assets and Transportadora de Gas del Sur S.A. for allowing the use of proprietary information.

References

- [1] ASME, SA-203/SA-203M, "Specification for Pressure Vessel Plates, Alloy Steel, Nickel", ASME II, Part A, Adenda, 2003.
- [2] Boiler and Pressure Vessel Code, ASME VIII, Division 1, Rules for Construction of Pressure Vessels, USA, 2010.
- [3] Report GIE 12-TGSAR-072012-008-01 Failure Analysis of Vessel 8-0302 A. TGS S.A. 2012 (in Spanish).

- [4] AWS A5.5/A5.5M: 2014, Specification for Low-Alloy Steel Electrodes for Shielded Metal Arc Welding, 2014.
- [5] AWS A5.11/A5.11M: 2010, Specification for Nickel and Nickel-Alloy Welding Electrodes for Shielded Metal Arc Welding, 2010.
- [6] Nickel Alloy Steel Plates, The international Nickel Company, Inc., 1972.
- [7] Low temperature properties of nickel alloy steels, The international Nickel Company, Inc., 1975.
- [8] Metals Handbook, Volume 9: "Metallography and Microstructure". ASM International, 9th ed, 1992 USA.
- [9] Damage mechanisms affecting fixed equipment in the refining industry, Recommended Practice 571, 1st edition American Petroleum Institute, 2003.
- [10] J.E. Shigley, Shigley's Mechanical Engineering Design, Tata Mc Graw-Hill Educ, 2011.
- [11] C. Guillaume, Invar and Elinvar, Nobel Lecture, December 1920.
- [12] S.R. Thorat, Y.R. Kharde**, K.C. Bhosale ***, S.B. Kharde, Effect of welding conditions on residual stresses and heat source distribution on temperature variations on butt welds: a review, *Int. J. Eng. Res. Appl.* 3–1 (2013) 1434–1439.
- [13] K. Behseta, D. Mackenzie, R. Hamilton, Ratcheting assessment of a fixed tube sheet heat exchanger subject to in phase pressure and temperature cycles, *J. Press. Vessel. Technol.* 133 (4) (2011) <http://dx.doi.org/10.1115/1.4003623> (5 pages).
- [14] U. Dilthey, Welding and Cutting Technologies, ISF Welding Institute and Aschen University, 2003.
- [15] O.A. El Kebi, A.A. Szummer, Comparison of hydrogen embrittlement of stainless steels and nickel-base alloys, *Int. J. Hydrog. Energy* 27 (2002) 793–800.
- [16] T. Michler, J. Naumann, Hydrogen environment embrittlement of austenitic stainless steels at low temperatures, *Int. J. Hydrog. Energy* 33–8 (2008) 2111–2122, <http://dx.doi.org/10.1016/j.ijhydene.2008.02.021>.
- [17] M.J. Cheaitani, R.J. Pargeter, Fracture Mechanics Techniques for Assessing the Effects of Hydrogen on Steel Properties, *Int'l Steel and Hydrogen Conf.*, Ghent, Belgium, Sept 2011.